Journal of the European Ceramic Society **17** (1997) 1231–1238

PII: S0955-2219(95)00221-X
0955-2219/96/$15.00

Sol–Gel Processing of PNZST Thin Films on Ti/Pt and Ta/Pt Metallizations

Cyril Voisard,[a] Keith G. Brooks,[a] Ian M. Reaney,[b] Laurent Sagalowicz,[a] Andrei L. Kholkin,[a] Nicolas Xanthopoulos[c] and Nava Setter[a]

[a]Laboratoire de Céramiques [c]Groupe de 'Analyse de Surface, EPFL, Ecublens, 1015 Lausanne, Switzerland
[b]Department of Engineering Materials, University of Sheffield, Sheffield, S14 0U, UK

(Received 13 June 1996; accepted 21 October 1996)

Abstract

Sol–gel processing parameters of $Pb_{0.99}Zr_{0.55}Sn_{0.37}Ti_{0.06}Nb_{0.02}O_3$ thin films were studied. Effects of H_2O, HNO_3 and formamide additives on solution gelation and film properties were investigated. Thin films were prepared on Ti/Pt and Ta/Pt metallized Si substrates. Film microstructures were characterized using SEM, TEM/EDS and XPS. Film microstructures typically contained 'rosette' structures. Strain response of the films under applied electric fields was measured using a double beam interferometer. A piezoelectric double loop was obtained with an effective d_{33} as high as 60 pm V^{-1}, being strongly AC field dependent. Double P-E hysteresis loops with maximum polarizations of 30 $\mu C\ cm^{-3}$ were measured. Field-induced antiferroelectric to ferroelectric phase switching was observed at 110 $kV\ cm^{-1}$ and reverse switching at 74 $kV\ cm^{-1}$. Films prepared on Ti/Pt yielded better electrical properties. This may be attributed to a change in nucleation/crystallization mechanism due to Pb diffusion through the Pt during film annealing. © *1996 Elsevier Science Limited.*

1 Introduction

The high piezoelectric coefficients of $Pb(Zr,Ti)O_3$ (PZT) bulk ceramics[1] coupled with advances in PZT thin film technology have spurred research into development of microactuators and sensors based on PZT thin films (e.g. micromotors,[2] pyroelectric detectors[3]). Compositional modification of PZT through Sn addition leads to the stabilization of an antiferroelectric tetragonal phase at room temperature for particular compositions[4,5] (Xu *et al.* describe this phase as an incommensurate orthorhombic one[6]). Because of the small free energy difference between the antiferroelectric and ferroelectric phases for compositions near the phase boundary, antiferroelectric to ferroelectric phase switching can be achieved upon application of an electric field.[7–10] It is particularly interesting for thin films where the required fields are obtained by applying small voltages. These materials exhibit the characteristic double hysteresis loop of antiferroelectrics. The large volume change associated with the phase transformation is high enough to be used for microactuators.[10]

Several methods are currently employed for the deposition of thin ceramic layers on substrates, including metal organic chemical vapour deposition (MOCVD),[11] physical vapour deposition (PVD), and wet chemical techniques such as sol–gel methods (using dip or spin coating). By PVD and MOCVD it is possible to grow thin films *in situ*; however the capital and operation costs are high and the systems are complex. On the other hand, sol–gel deposition offers a cost-effective approach. Using sol–gel techniques, film composition can be changed easily, to allow for the addition of dopants, for example. However, the crystallization of the films is *ex situ*, thus requiring efficient nucleation to obtain controlled microstructures and reproducible properties.

During the crystallization of amorphous sol–gel films, the properties of the substrate play an important role. The temperature of the annealing process is limited by the stability of the Pt and Pt adhesion layer(s) at temperatures above 700°C. Pb loss during film annealing and Nb content also play a significant role in determining the occurrence of a residual pyrochlore phase.[12] For materials like PNZST and PMN, for which the pyrochlore phase is very stable, annealing temperatures of the order of 800°C are commonly employed.[13] Chen *et al.* have shown that the use of rapid thermal annealing can lead to improved film quality.[14] The perovskite nucleation process is influenced by a number of parameters, including the free energy

of each phase appearing during the crystallization (amorphous, pyrochlore and perovskite), the number of nucleation sites and lowering of the interfacial energy through epitaxial growth mechanisms (e.g. PZT (111) and Pt (111)).[15] Several authors have reported that a nanocrystalline pyrochlore type phase forms before nucleation of perovskite structured grains during annealing. Nucleation of perovskite grains is often reported to begin at the Pt/PZT interface. The grains then grow towards the free surface of the film creating a columnar morphology. The texture/orientation of the film has been shown to depend strongly on the pyrolysis conditions, with orientations ranging from (100) to (111) to random depending on pyrolysis temperature.[15]

For sol–gel preparation, the thin film properties are dependent on the precursor solution characteristics.[16,17] These properties result from several chemical reactions which occur in the solution during the processing, namely hydrolysis and condensation of the organo-metallic species. It has been shown for tetraethoxysilane (TEOS) that additives can be used to modify the thin film properties.[18] However, multicomponent PNZST sol solutions are by far more complicated (in terms of reaction kinetics, etc.) than TEOS ones.

The effect of hydrolysis on the preparation of Pb-containing perovskite thin films has been studied by several groups.[16,18–20] Budd *et al.* have shown that increasing the quantity of water in the precursor solution causes acceleration of the gelation kinetics.[16] Lipeles *et al.* reported that the introduction of a large quantity of water led to porous and partially crystallized PZT films.[19] Acids and bases change both the hydrolysis and condensation rates, and thus affect the structure of the condensed gel.[18] For TEOS, the chemical species are much more cross-linked in an alkaline medium than in an acidic one where the oligomers are roughly linear.[18] This paper reports on the deposition of $Pb_{0.99}Zr_{0.55}Sn_{0.37}Ti_{0.06}Nb_{0.02}O_3$ (PNZST) thin films by a sol–gel method on Si substrates with two different types of bilayer metallization: Ti/Pt and Ta/Pt. For the films deposited on Ta/Pt type substrate, chemical additives including H_2O, HNO_3 and formamide were used to modify the sol–gel precursor solutions, and thus influence the microstructural and electrical properties of the films.

2 Experimental Procedure

2.1 Sol–gel investigations

The proximity of the PNZST composition investigated to the antiferroelectric–tetragonal ferroelectric rhombohedral phase boundary is shown in the room temperature phase diagram for the system $PbTiO_3$–$PbZrO_3$–PbO:SnO_2 (Fig. 1.; after Berlincourt[9]). Sol–gel precursor solutions were made using reagent grade lead acetate trihydrate, tin acetate, titanium isopropoxide, zirconium *n*-propoxide and niobium ethoxide. The solvent was anhydrous 2-methoxyethanol. According to a previously reported procedure,[21] lead acetate trihydrate was refluxed 8 h at 350 mbar and 80°C, and then distilled to remove the water of hydration. Next, the Pb acetate solution was refluxed for 2 h using the same conditions as above. A separate solution containing the Ti, Zr, Sn and Nb precursors in 2-methoxyethanol was prepared in a dry nitrogen glove box. This solution was then added to the distilled Pb acetate solution. The resulting solution was refluxed for 2 h at 110°C and 350 mbar. Finally, the solution concentration was adjusted by distillation and a drying control chemical additive (formamide, NH_2CHO) was used to stabilize the solution against hydrolysis and prevent crack formation during thin film preparation.

The partial hydrolysis of the solution was performed with different molar ratios of water (R_w) or nitric acid (R_A) to PNZST. Gelation kinetics have been studied by measuring the time elapsed between hydrolysis and gelation steps. The partially hydrolysed solutions were aged at 70°C to increase the rate of gelation. The gels were dried on a hot plate and then characterized using XRD and SEM.

2.2 Thin film investigations

Two different types of Pt-metallized Si wafers were used for the deposition of the PNZST thin films. The first type was commercially supplied and consisted of Si wafers with 1 μm of SiO_2, 10 nm Ti and 100 nm Pt. The second variety was prepared in our laboratory and consisted of PVD-deposited Ta/Pt (10 nm/100 nm) on Si/SiO_2 substrates. Thin films were deposited by spin coating the precursor solution at 3000 rpm for 30 s followed by pyrolysis at 350°C for 15 s. Annealing was performed using a rapid thermal annealing furnace with flowing oxygen. Platinum top electrodes were deposited by sputtering.

Film crystallinity and microstructure was investigated by X-Ray diffraction using a standard Cu K_α = 1·54 Å cathode, scanning electron microscopy (SEM) and transmission electron microscopy (TEM). TEM observations were performed on transverse sections. Details of the TEM sample preparation have been previously reported.[22] Energy Dispersive Spectroscopy (EDS) results were obtained with a field emission gun operated at 200 kV. The different layers were analysed with a probe size of about 2 nm. Film compositions as a function of

Table 1. Gelation time measurements in hours for the partially hydrolysed PNZST solutions for two solution concentration (0·4 M and 0·6 M)

$[H_2O/PNZST]$	c=0·6 M	c=0·4 M
4	288	—
6	84	279
8	—	71
10	—	63

thickness were investigated by X-ray photoelectron spectroscopy (XPS) using a 350 W Mg anode.

Hysteresis loops were measured using a standard commercial test equipment and strain response measured using a double beam interferometer.[23] Relative permittivity as a function of DC bias field was measured with an impedance gain phase analyser.

3 Results and Discussion

3.1 Hydrolysis and gelation time measurement

The dependence of the gelation time on quantity of added water is summarized in Table 1. Increasing the quantity of water is observed to decrease the gelation time exponentially.

During the gelation time study, precipitation of lead formate crystals[24] has been observed for different hydrolysis and aging conditions. First, at high quantities of water (R_W = 6), gelation occurs rapidly and no precipitation is observed. The XRD pattern, Fig. 2, shows only a broad low intensity peak indicating an amorphous phase. Second, when the quantity of water is low (R_W = 2), the solution remains stable (does not gel) for at least four months. However, after several weeks, large (mm size) lead formate single crystals are observed to form, Fig. 3. In between these two cases, for R_W = 4, gelation and crystallization of lead formate occur simultaneously, Fig. 2. From this figure, it is obvious that the acid content has no significant effect on the crystallinity of the dried gels. The formation of Pb formate is interesting because its presence will cause the gelled material to be lead-deficient (with respect to PNZST stoichiometry) thus leading to chemical inhomogeneity in the sol–gel films. The following chemical reaction mechanism is proposed: formamide is hydrolysed producing formic acid which then reacts with lead acetate to form lead formate (described by Brinker and Scherer[18]).

The influence of the sol–gel additives on the nucleation, crystallization and electrical properties of the PNZST thin films is discussed below.

3.2 Film deposition on Ti/Pt type substrates

For all of the films prepared on Ti/Pt type substrates, no water or acid was added. The SEM micrograph presented in Fig. 4(a) shows the surface of a PNZST film prepared on Ti/Pt metallization. The microstructure is characterized by perovskite rosettes (gray features) embedded in a nanocrystalline pyrochlore phase (dark regions). The size distribution of the rosettes is bimodal, with mean diameters of about 1 μm and 0·5 μm. A TEM micrograph of part of a transverse section of a PNZST film on Ti/Pt metallization is shown in Fig. 5(a). This micrograph indicates that nucleation begins at the Ti/Pt interface. All of the films prepared on Ti/Pt substrate were strongly [111] oriented.

A characteristic double P/E hysteresis loop was observed in the case of films deposited on Ti/Pt, Fig. 6. This film was 295 nm thick and was annealed at 750°C for 30 s. A maximum polarization value of 30 μC m^{-2} was measured. Switching threshold fields from the antiferroelectric phase to

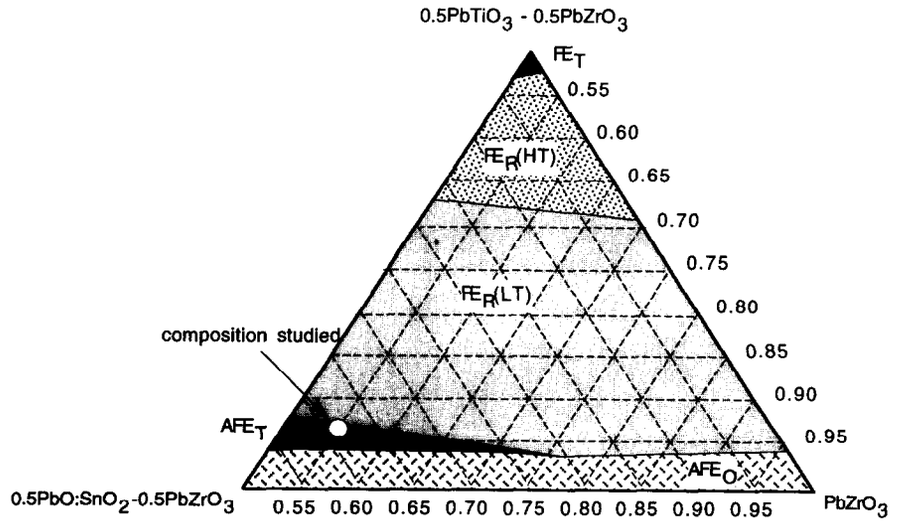

Fig. 1. Room-temperature phase diagram of $PbZrO_3$–$PbTiO_3$–$PbO:SnO_2$ ternary system with the location of the composition studied indicated.[9]

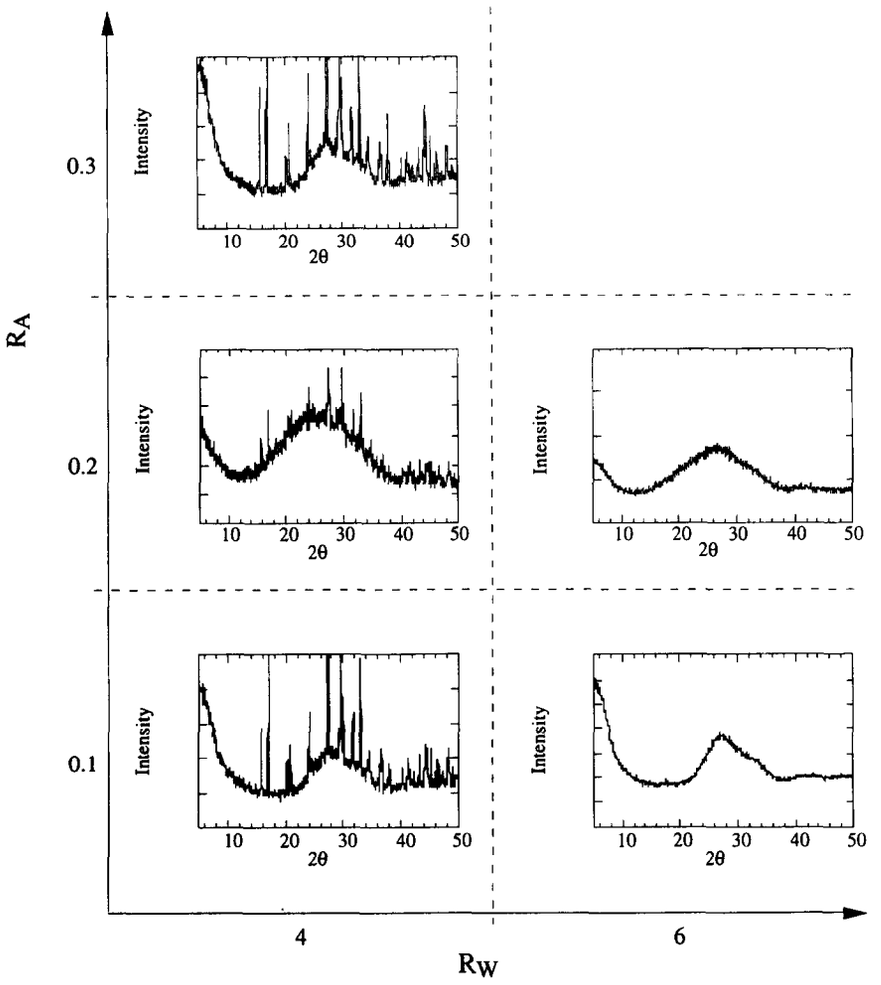

Fig. 2. X-ray diffraction patterns of dried gels prepared with formamide addition and different molar ratios of water (R_W) or acid (R_A). The gels are fully amorphous for R_W=6 so no sharp diffraction peaks are visible, just a broad amorphous peak. Several diffraction peaks can be seen for R_W=4, all of them belonging to lead formate, JPDS file number 14-825. Acid content does not affect the crystallinity of the gels.

the ferroelectric phase as determined from relative permittivity versus DC electrical field measurements are 110 kV cm^{-1} and 74 kV cm^{-1}, for forward and reverse switching, respectively. The dielectric constant is about 460 at zero bias field and about 660 at the phase transitions, for measurements at 50 mV and 10 kHz.

3.3 Film deposition on Ta/Pt type substrates

The hysteresis loops of films prepared from partially hydrolysed and non-hydrolysed solutions with all other parameters held constant on a Ta/Pt type substrate are presented in Fig. 7. In the case of the pre-hydrolysed solution, the film was deposited 5 min after hydrolysis. The annealing temperature was 650°C during 5 min. By comparison with the hysteresis data for films prepared without H_2O, it is clear that pre-hydrolysis of the precursor solution destroys the electrical properties of the film as previously observed in PZT thin films (see, for example, Ref. 19). By storing the hydrolysed solution at 0°C prior to film deposition, however, it was possible to maintain the properties of the films constant (i.e. slow down the hydrolysis reaction). These two observations indicate that careful control of the water content of the precursor solutions and the relative humidity are critical for the preparation of high quality PNZST thin films. Films prepared with no water or acid additions to

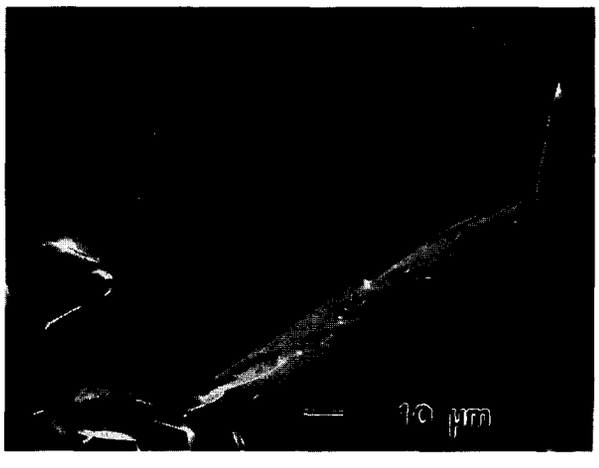

Fig. 3. SEM photomicrograph of a lead formate single crystal nucleated inside a precursor solution.

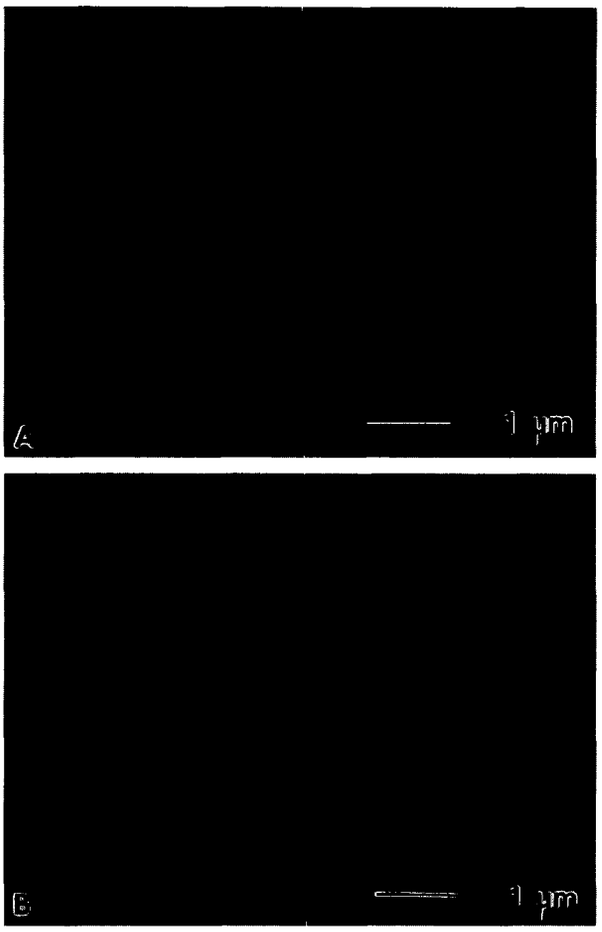

Fig. 4. SEM photomicrograph of the surface of a PNZST film prepared on (a) Ti/Pt and (b) Ta/Pt metallization.

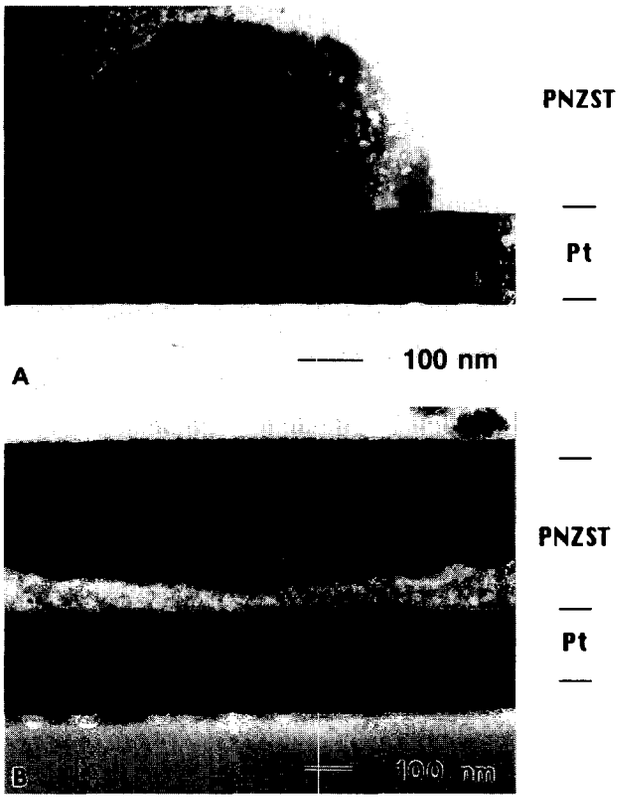

Fig. 5. TEM images of transverse sections of PNZST films prepared on (a) Ti/Pt and (b) Ta/Pt metallization. For both pictures the substrate is at the bottom and the free surface at the top.

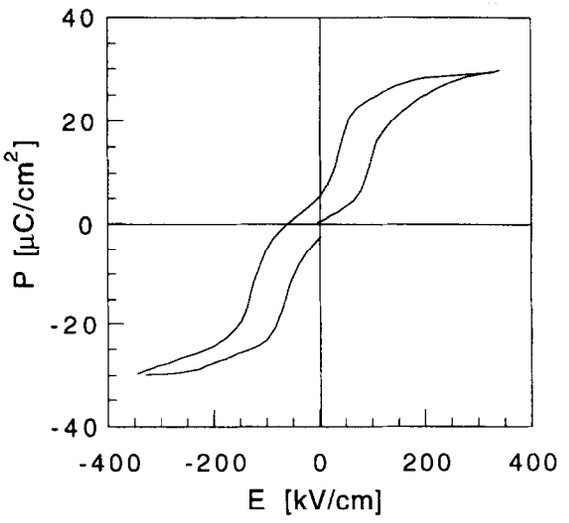

Fig. 6. Polarization-electric field hysteresis loops of a PNZST thin film prepared on a Ti/Pt electrode.

the sol–gel precursors were investigated in more detail, as discussed below.

The nucleation rate of PNZST on the Ta/Pt substrate is lower compared to the Ti/Pt case, as can be seen in the SEM micrograph of Fig. 4(b). The number of rosettes per unit area is diminished. The rosettes are regularly shaped with large lateral dimensions (about 1 μm). In Fig. 4(b), a straight grain boundary between two grains can be seen where the two grains have impinged during lateral growth, a typical feature of rosette type grain growth.[25] For the PNZST films deposited on Ta/Pt, the perovskite nucleation did not initiate as expected at the film–Pt interface, but near the film surface, indicating that nucleation at the film–Pt interface is somehow inhibited compared to Ti/Pt. The surface nucleated grains have grown towards the bottom electrode, as evidenced in the TEM micrograph, Fig. 5(b). Close to the film–Pt interface,

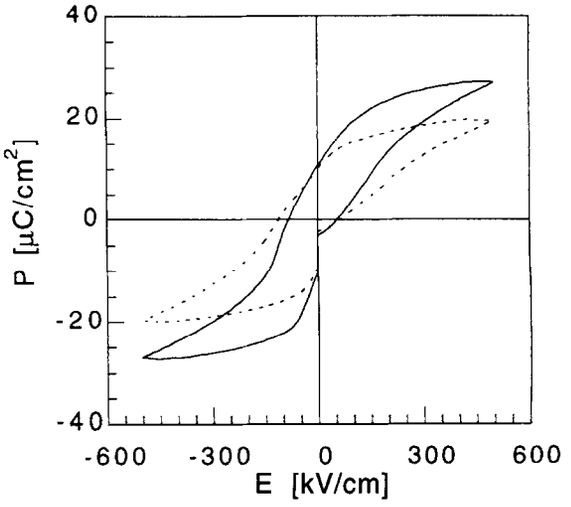

Fig. 7. Polarization-electric field hysteresis loops obtained from PNZST thin films prepared from a pre-hydrolysed (dashed line) and non-hydrolysed precursor solution (solid line).

Table 2. EDS quantitative analyses performed on a PNZST thin film deposited on a Ta/Pt substrate. The quantity of each element is expressed in atomic percent

Probe position	*Pb*	*Zr*	*Ti*	*Sn*	*Nb*
Perovskite	51 ± 4	23 ± 2	3 ± 1	22 ± 1	0·4 ± 0·3[a]
Pyrochlore	31 ± 4	33 ± 3	3 ± 1	30·5	2 ± 2[a]

[a]Due to the low amount of Nb and to the high K factor of this element, a large uncertainity is associated with the quantification.

no nucleation has been observed and most of the time the pyrochlore remains. The films were [111] textured as observed by XRD. The composition of the perovskite phase in cation percent (Table 2) was found to be: Pb=51, Nb=0·4, Zr=23, Sn=22, Ti=3, which is near the nominal composition. The pyrochlore region was found to have a similar composition except that it was poorer in Pb (atom% Pb=30). To obtain these results, thicker sample regions were used. EDS analysis on bulk PZT indicates that for such large thicknesses analyses are precise and accurate within 10%. A large amount of Pb (about 30% in atomic percent in the Ta), which had diffused through the Pt during rapid thermal annealing of the film, was observed in the Ta layer. This created Pb deficiency at the bottom of the film which may prevent perovskite nucleation by changing the relative stabilities of the pyrochlore and the perovskite phase. Further quantitative analysis by means of EDS and XPS surface analysis has indicated that Ta diffuses through the Pt layer during film annealing. The XPS depth profile, Fig. 8, indicates that the Ta distribution is significantly shifted towards the film–Pt interface. EDS spectra were obtained from a Pt grain boundary, Fig. 9 (a), and inside a Pt grain, Fig. 9 (b). There is evidence of Ta enrichment in the Pt grain boundary. By EDS, no direct

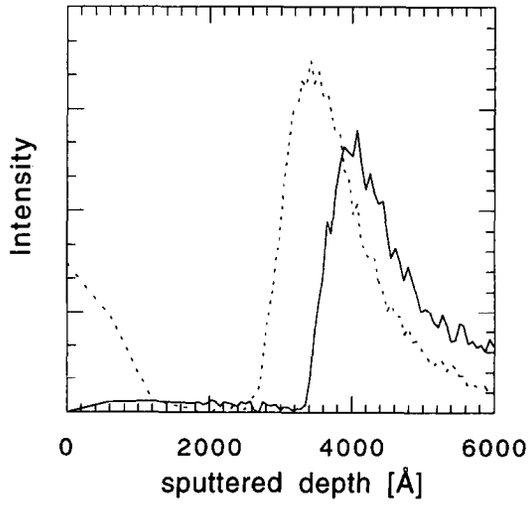

Fig. 8. XPS depth profile showing a shift of Ta distribution towards the film–Pt interface, the solid line corresponds to the Ta profile and the dashed one to the Pt profile.

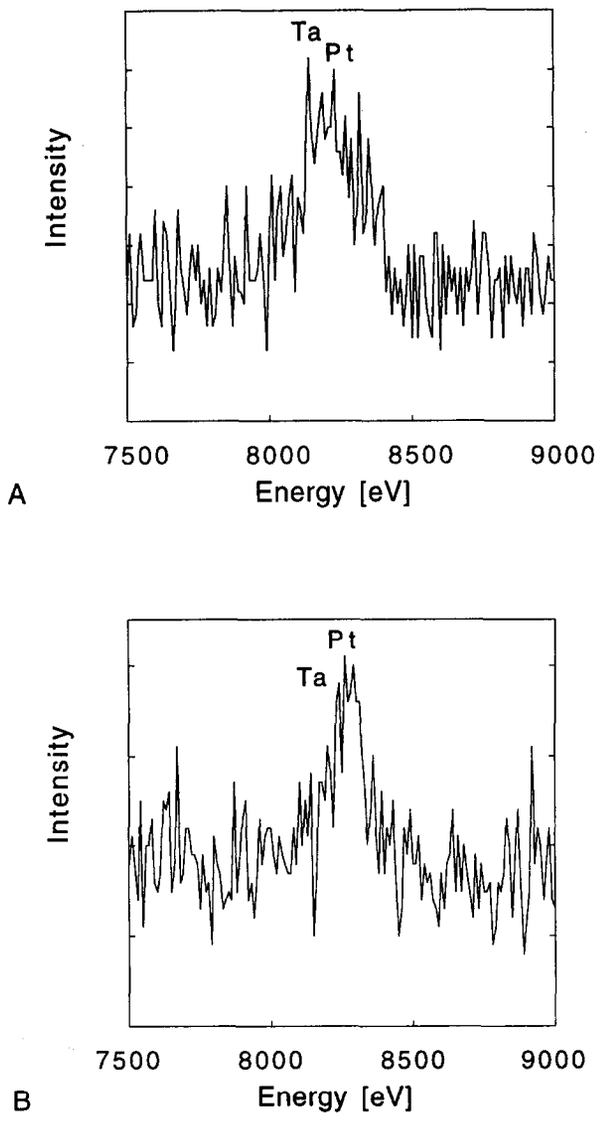

Fig. 9. EDS spectrum of (a) a Pt grain boundary and (b) inside a Pt grain indicating diffusion of Ta during the annealing process. Corresponding characteristic energies are for Ta ($L\alpha_1$): 8145 eV and for Pt ($L\lambda$): 8267 eV.

proof of Ta enrichment at the film–Pt interface could be obtained. This is not surprising since a small content (about 1 at (%) would not be detected due to noise and screening from other elements. The nucleation inhibition at the film–Pt interface may be explained as follows. The primary reason is that a significant quantity of Pb diffuses through the Pt into the Ta layer, thus causing a Pb deficiency in the film at the film–Pt interface and inhibiting nucleation of the perovskite structure. In addition, Ta diffuses through Pt during the annealing process and the presence of Ta oxide at the interface could inhibit the perovskite nucleation because Ta is known to form stable pyrochlore phases.[26]

3.4 Electric field-induced strain in PNZST films

Figure 10 shows the effective piezoelectric coefficient d_{33} of a PNZST film deposited on a Pt/Ti substrate as a function of DC electric field. At low

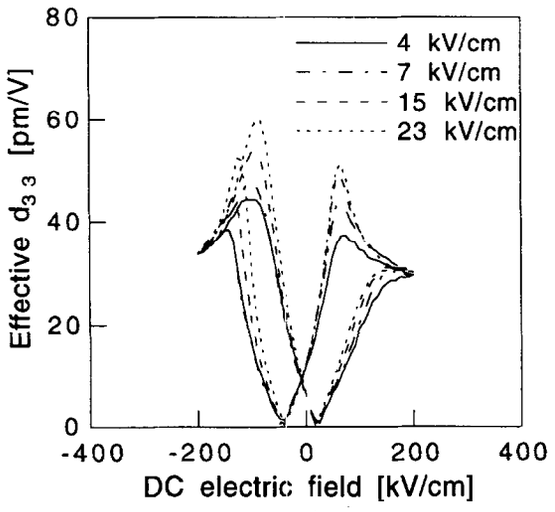

Fig. 10. Effective piezoelectric coefficient of a PNZST film deposited on a Ti/Pt substrate as a function of DC electric field.

electric field (in the antiferroelectric state) d_{33} is small (5–10 pm V^{-1}) and then significantly increases when switching to the ferroelectric state occurs at higher fields. A strong dependence of d_{33} on the AC field level is found near the switching threshold field where a relatively small AC field can induce large strains. Under the strong DC field this dependence is almost absent since ferroelectric domains are aligned in the direction of the applied electric field and domain wall motion contribution is reduced. The piezoelectric coefficient of about 60 pm V^{-1} is obtained near the switching field to ferroelectric state. This value is similar to that obtained by Gaskey *et al.*[6] in PNZST films of composition $Pb_{0.99}Nb_{0.02}Zr_{0.85}Sn_{0.13}Ti_{0.02}O_3$ under the same electric field. A significant asymmetry of the piezoelectric response is found suggesting non-equivalent conditions for the ferroelectric phase at positive and negative directions of applied field. This may be a result of a non-uniform charge distribution and internal bias field in the PNZST film due to pyrochlore phase and compositional differences. Figure 11 shows the strain versus field dependencies of the same film measured at different AC fields. At a driving field of about 200 kV V^{-1}, which only slightly exceeds the switching field, the strain is found to increase significantly under switching to the ferroelectric state. The remanent strain is much smaller than the maximum strain in accordance with polarization measurements. A stronger asymmetry of the strain response is observed compared to the d_{33} measurements. At higher driving fields stabilization of the ferroelectric state results in a strong increase of the remanant strain as compared to the low field conditions. Therefore a complete recovery of the antiferroelectric state could not be seen. This is understood as a result of the shift of the phase boundary between ferroelectric rhombohedral and antiferroelectric

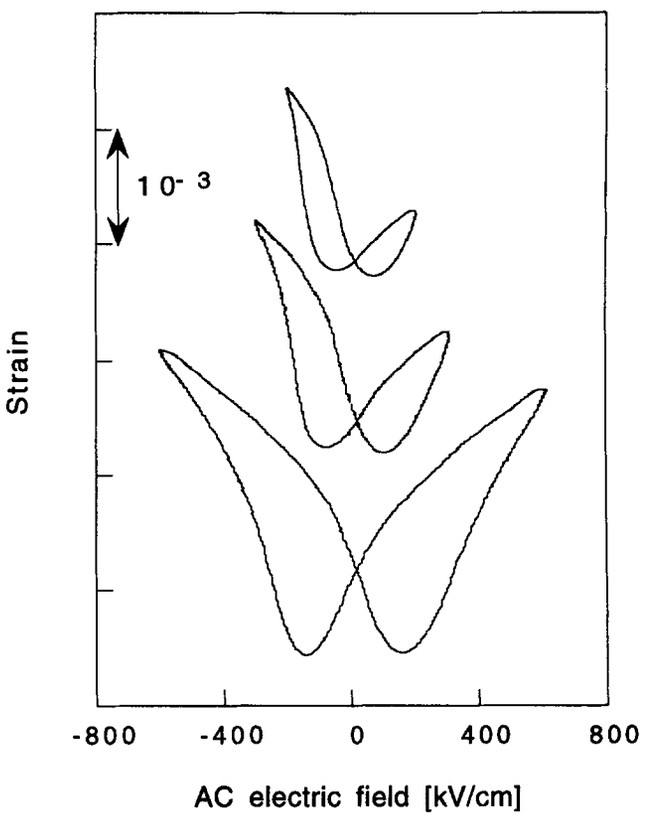

Fig. 11. Strain versus electric field measurement of a PNZST thin film prepared on a Ta/Pt electrode.

tetragonal phases under the high electric field used for the strain measurements.[8] The longitudinal strain is about 0·25% under an electric field of 600 kV V^{-1}.

4 Conclusions

Nucleation and growth of lead formate were observed in PNZST sol–gel precursor solution. Hydrolysis parameters (water and nitric acid molar ratios) influence the conditions of growth of lead formate.

Antiferroelectric PNZST films which show well-defined antiferroelectric to ferroelectric electric field forced phase switching were prepared on Ti/Pt-metallized Si wafers. For the films on Ti/Pt, nucleation occurs at the film–Pt interface, and a columnar microstructure is obtained. On Ta/Pt, nucleation occurs at the film surface. Pb diffusion through the Pt bottom electrode could explain this change. The films on Ti/Pt substrates exhibit promising electromechanical properties for actuator applications.

5 Acknowledgements

The authors would like to acknowledge Marija Kosek for helpful discussions. TEM work was

performed at the CIME (EPFL). This work, part of a diploma project, was funded by the Swiss Federal Institute of Technology, Lausanne, Switzerland.

References

1. Jaffe, B., Cook, W. R. and Jaffe H., *Piezoelectric Ceramics.* Academic Press, London, 1971.
2. Muralt, P. *et al.*, Fabrication and characterization of PZT thin-film vibrators for micromotors. *Sensors and Actuators A*, 1995, **48**, 157–165.
3. Kohli, M. *et al.*, Processing and properties of thin film pyroelectric devices. *Microelectronic Engng*, 1995, **29**, 93–96.
4. Jaffe, B., Roth, R. S. and Marzullo, S., Properties of piezoelectric ceramics in the solid solution series lead titanate zirconate—lead oxide: tin oxide and lead titanate—lead hafnate. *J. Res. Nat Bureau Stand.*, 1995, **55**(5), 239–255.
5. Gaskey, C. J. *et al.*, 'Square' hysteresis loops in phase-switching Nb-doped lead zirconate stannate titanate thin films. *J. Mater. Res.*, 1995, **10**(11), 2764–2769.
6. Xu, Z., Viehland, D. and Payne, D. A., An incommensurate-commensurate phase transformation in antiferroelectric tin-modified lead zirconate titanate. *J. Mater. Res.*, 1995, **10**(2), 453–460.
7. Yang, P. and Payne, D. A., Thermal stability of field-forced and field-assisted antiferroelectric–ferroelectric phase transformations in $Pb(Zr,Sn,Ti)O_3$. *J. Appl. Phys.*, 1992, **71**(3), 1361–1367.
8. Berlincourt, D., Krueger, H. H. A. and Jaffe, B., Stability of phases in modified lead zirconate with variation in pressure, electric field, temperature and composition. *J. Phys. Chem. Solids*, 1964, **25**, 659–674.
9. Berlincourt, D., Transducers using forced transitions between ferroelectric and antiferroelectric states. *IEEE Trans. on Sonics and Ultrasonics*, 1966, **SU-13**(4), 116–125.
10. Pan, W. Y. *et al.*, Large displacement transducers based on electric field forced phase transition in the tetragonal $(Pb_{0.97}La_{0.02})(Ti, Zr, Sn)O_3$ family of ceramics. *J. Appl. Phys.*, 1989, **66**(12), 6014–6023.
11. Keijser, M. S., Organometallic chemical vapour deposition of lead zirconate titanate. PhD thesis, Eindhoven, Philips Research Laboratories, 1995.
12. Klissurska, R. D. *et al.*, Effect of Nb doping on the microstructure of sol–gel-derived PZT thin film. *J. Am. Ceram. Soc.*, 1995, **78**(6), 1513–1520.
13. Francis, L. F. and Payne, D. A., Processing, perovskite phase development and dielectric properties for sol–gel-derived $Pb[(Mg_{1/3}Nb_{2/3})_{0.9}Ti_{0.1}]O_3$ thin layers. *Mater. Res. Soc. Symp. Proc.*, 1990, **200**, 173.
14. Chen, J. *et al.*, Rapid thermal annealing of sol–gel-derived zirconate titanate thin films. *J. Appl. Phys.*, 1992, **71**(9), 4465–4469.
15. Brooks, K. G. *et al.*, Orientation of rapid thermally annealed lead zirconate titanate thin films on (111) Pt substrates. *J. Mater. Res. Soc.*, 1994, **9**(10), 2548–2553.
16. Budd, K. D., Dey, S. K. and Payne, D. A., The effect of hydrolysis conditions on the characteristics of $PbTiO_3$ gels and thin films. *Mater. Res. Soc. Symp Proc.*, 1986, **73**, 711–716.
17. Lakeman, C. D. *et al.*, An investigation into the factors affecting the sol–gel processing of PZT thin layers. *IEEE 7th International Symposium Applied Ferroelectrics*, 1990, 681–684.
18. Brinker, C. J. and Scherer, G. W., In *Sol-Gel Science, The Physics and Chemistry of Sol-Gel Processing.* A. P. Inc., Ed., 1990, p. 130.
19. Lipeles, R. A., Coleman, D. J. and Leung, M. S., Effects of hydrolysis on metallo-organic solution deposition of PZT films. In *Better Ceramics through Chemistry II* eds C. J. Brinker, D. E. Clark, D. R. Ulrich. Material Research Society, Pittsburgh, Pennsylvania, 1986, pp. 665–670.
20. Schwartz, R. W. *et al.*, Solution chemistry effects in $Pb(Zr, Ti)O_3$ thin film processing. *Integrated Ferroelectrics*, 1990, **2**, 153–158.
21. Brooks, K. G. *et al.*, Electric field forced antiferroelectric to ferroelectric phase switching in sol–gel-derived $(Pb_{0.97}La_{0.22})$ $(Zr,Ti,Sn)O_3$ thin films. *J. Appl. Phys.*, 1994, **75**(3), 1699.
22. Reaney, I. M. *et al.*, Use of transmission electron microscopy for the characterization of rapid thermally annealed solution—gel, lead zirconate titanate films. *J. Am. Ceram. Soc.*, 1994, **77**(5), 1209–1216.
23. Kholkin, A. L. *et al.*, Interferometric measurements of electric field-induced displacements in piezoelectric thin films. *Rev. Scient. Instrum.*, 1996, **67**(5), 1935–1941.
24. Harrison, P. G. and Steel, A. T., Lead(II) carboxylate structures. *J. Organometallic Chemistry*, 1982, **239**, 105–113.
25. Myers, S. A. and Chapin, L. N., Microstructural characterization of ferroelectric thin films for non-volatile memory applications. *Mater. Res. Soc. Symp. Proc.*, 1990, **200**, 153–158.
26. Subramanian, M. A., Aravamudan, G. and Rao, G. V. S., Oxide pyrochlores — A *review. Prog. Solid St. Chem.*, 1983, **15**, 55–143.